ACS OMEGA

http://pubs.acs.org/journal/acsodf

Article

# Enhanced Fluorescence and Environmental Stability of Red-Emissive Carbon Dots via Chemical Bonding with Cellulose Films

Yeqing Chen,* Gaoyang Xiong, Lina Zhu, Jie Huang, Xueying Chen, Yan Chen, and Mingxuan Cao*

Cite This: *ACS Omega* 2022, 7, 6834−6842

Read Online

ACCESS | Metrics & More | Article Recommendations | Supporting Information

**ABSTRACT:** The development of red emission carbon dots with bright solid-state fluorescence would significantly broaden their application in optoelectronic devices and sensors. Herein, a red-emissive carbon dot-based nanocomposite has been synthesized through chemical bonding with cellulose films. The red emission originating from the surface states of carbon dots was maintained in the cellulose films. Due to the stable chemical bonding, the photoluminescence intensity and emission wavelength remained unchanged for 12 months, and the quantum yield of the composite was enhanced over 4 times. It also showed outstanding stability in water or weak acid−base environments under pHs ranging from 2 to 11. Therefore, the mechanism of chemical bonding that eliminated the defects and preserved the efficient radiative process through surface states was proposed.

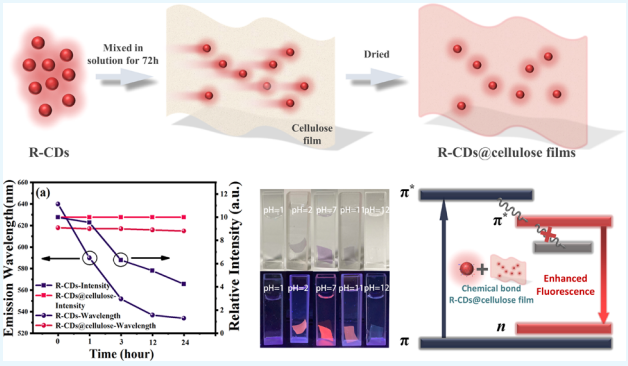


## 1. INTRODUCTION

Over the past decade, carbon dots (CDs) have been extensively investigated as fluorescent nanomaterials due to their unique optical properties[1−5] and advantage in optoelectronic devices,[6,7] bioimaging,[8,9] and fluorescent sensing.[10] Many researchers have reported carbon dots with high photoluminescence quantum yield (PLQY) in blue and green spectral regions.[11] However, preparing the bright red emission of carbon dots was still a challenge, which was restricted by the lack of an effective synthesis method as well as a definite fluorescence mechanism.[12] Most of the carbon dots reported had bright emission in solution, while condensed CDs suffered a decrease in intensity or even quenching in the solid state. This aggregation-caused quenching (ACQ) phenomenon was due to the energy consumption within the conjugated $\pi$-domains.[13]

General methods of embedding the fluorescent centers in solid matrices, such as starches, inorganic minerals, and various polymers, have been carried out to enhance the photoluminescence properties. In the latest reports, a physical blending of the highly efficient red-emissive CDs with starch particles was carried out to form R-CDs/starch phosphors for latent fingerprints.[14] Also, inorganic minerals of mesoporous aluminas (MAs) were applied as a substrate to combine with carbon dots.[15] Two kinds of carbon dots were restricted within the substrate pores after stirring with MAs, and emissions originating from both blue and red CDs were retained. The hybrid material was applied as an oxygen sensor due to the monotonic quenching of red emission when it encountered oxygen, which also indicated that the carbon dots were unstable in the matrix with weak physical force. Moreover, the solid-state fluorescence of CDs could also be realized by hydrogen bonds when CDs were confined inside the space of polymer chains such as branched polyethyleneimine (PEI), poly(vinylpyrrolidone) (PVP), or polystyrene (PS), etc.[16−20] Although the inorganic minerals or organic matrix facilitated the nonradiative pathway between the fluorescent centers of CDs, the CD-based hybrid phosphors still had instability issues. When CDs were physically blended into substrates or polymer chains, they would still face the quenching problem in water, acids, or alkali environments due to weak physical bonds or space confinement.[21,22]

Nevertheless, establishing a chemical bonding between carbon dots and a matrix proved to be a more effective way for CD photoluminescence. Qu exploited chemical reactions between TEOS and carbon dots by generating a chemical bonding of Si−O to develop green-emitting composites, utilizing the functional groups on the surface of CDs, realizing high photoluminescence quantum yields over 40%.[23] Inorganic minerals such as $BaSO_4$ were reported as a suitable matrix material for carbon nanodots (CNDs), and electrostatically assembled hybrid phosphors CNDs@$BaSO_4$ were formed

**Received:** November 15, 2021
**Accepted:** February 8, 2022
**Published:** February 17, 2022





https://doi.org/10.1021/acsomega.1c06426
*ACS Omega* 2022, 7, 6834−6842

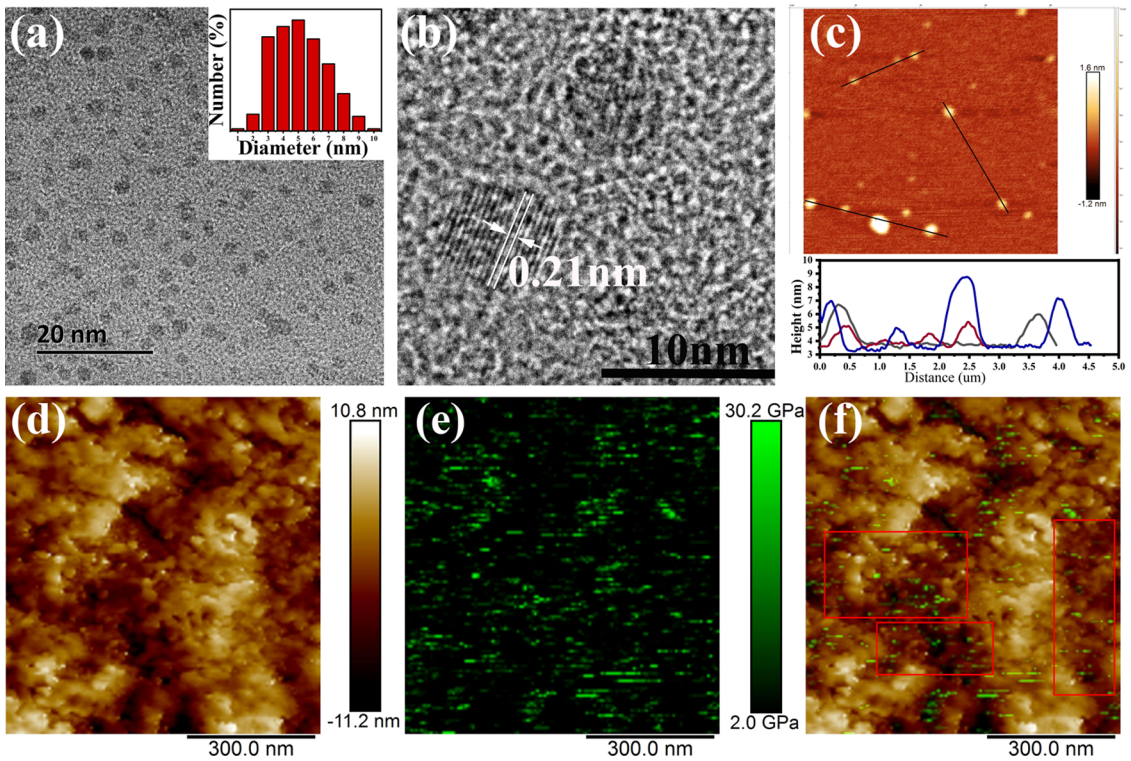


**Figure 1.** TEM image of (a) R-CDs and histogram of particle-size distribution (inset). (b) HRTEM image of a single carbon dot particle. (c) AFM height image of R-CDs and the height-profile analysis along the corresponding line. (d) Height image and (e) DMT modulus maps of R-CD@cellulose films and (f) merged image of both modes.

rather than through physical adsorption, leading to an enhanced green emission with a PLQY of 27%.[24] Moreover, Liu's group developed a sol−gel strategy using biowaste rice husk with high hydrocarbon and silica content as precursors, whose intermediate products sodium silicate played an important role in forming a compact 3D Si−O network. As is well accepted in the community, the enhancement of phosphorescence is always ascribed to the stabilized excited triplet states through hydrogen bonds. In this case, the CDs were connected to the Si−O network, the excited triplet states were rigidified, and the enhancement of phosphorescence was ascribed to the transition from a weak hydrogen bond to a strong covalent bond between CDs and the $SiO_2$ matrix.[25] However, the significance of forming a chemical bond between carbon dots and the matrix was neglected in many cases, while the enhancement of long-wavelength fluorescence CDs was rare.

It has been widely accepted that the surface-related states were responsible for the long-wavelength emission of CDs, while the hydroxyl bond or dangling bonds serving as nonradiative recombination centers were the main reason for the quenching of long-wavelength emission. Cellulose acetate films as one of the chemically modified natural polymers with outstanding transparency and environmental stability were well suited to be used as a carrier matrix combined with carbon dots due to the regularly distributed carboxyl groups, which provided the abundant binding sites for CD docking.

Herein, we reported a simple method to synthesize red-emissive carbon dots (R-CDs) by a hydrothermal process and combined the prepared R-CDs with regenerated cellulose acetate films through chemical bonding. The carbon dots combined with cellulose films (R-CDs@cellulose) show a 620 nm bright red fluorescence under ultraviolet (UV) with an excitation-independent feature. The PLQY was improved over 4 times through recombination, and the poor stability of R-CDs was greatly improved. The fluorescence properties of R-CDs@cellulose films can be maintained in open air for more than 1 year without degradation. And the R-CDs@cellulose films expressed excellent stability either in water or a weak acid−base environment.

## 2. EXPERIMENTAL SECTION

**2.1. Materials and Reagents.** Citric acid monohydrate (A.R.), ethanol (A.R.), and formamide (A.R.) were purchased from the Beijing Chemical Company. Regenerated cellulose acetate films were purchased from Shanghai Green Bird Company. Deionized water (DI) with a resistivity of 18.2 mΩ·cm was used in the experiments.

**2.2. Synthesis of Red-Emissive Carbon Dots.** R-CDs were synthesized via a hydrothermal method using citric acid and formamide as precursors.[26] In a general process, 0.02 mol of citric acid was dissolved in 15 mL of ethanol solvent under vigorous stirring with a magnetic bar for 15 min until a clear liquid was obtained. Fifteen milliliters of formamide was then added to the mixed solution with continuous stirring for 30 min. The solution was finally sealed in a 50 mL Teflon autoclave and heated at 160 °C for 8 h. The resulting dark solution was directly subjected to dialysis (cutoff molecular weight of 1000 Da, Shanghai Green Bird Company) for 3 days to remove the unreacted precursor and small molecular products, followed by freeze-drying; an orange-red solid was obtained, denoted R-CDs.

**2.3. Fabrication of Carbon Dots Recombined with Cellulose Films (R-CDs@Cellulose).** The regenerated cellulose acetate films were divided into rectangles with their



https://doi.org/10.1021/acsomega.1c06426
ACS Omega 2022, 7, 6834−6842

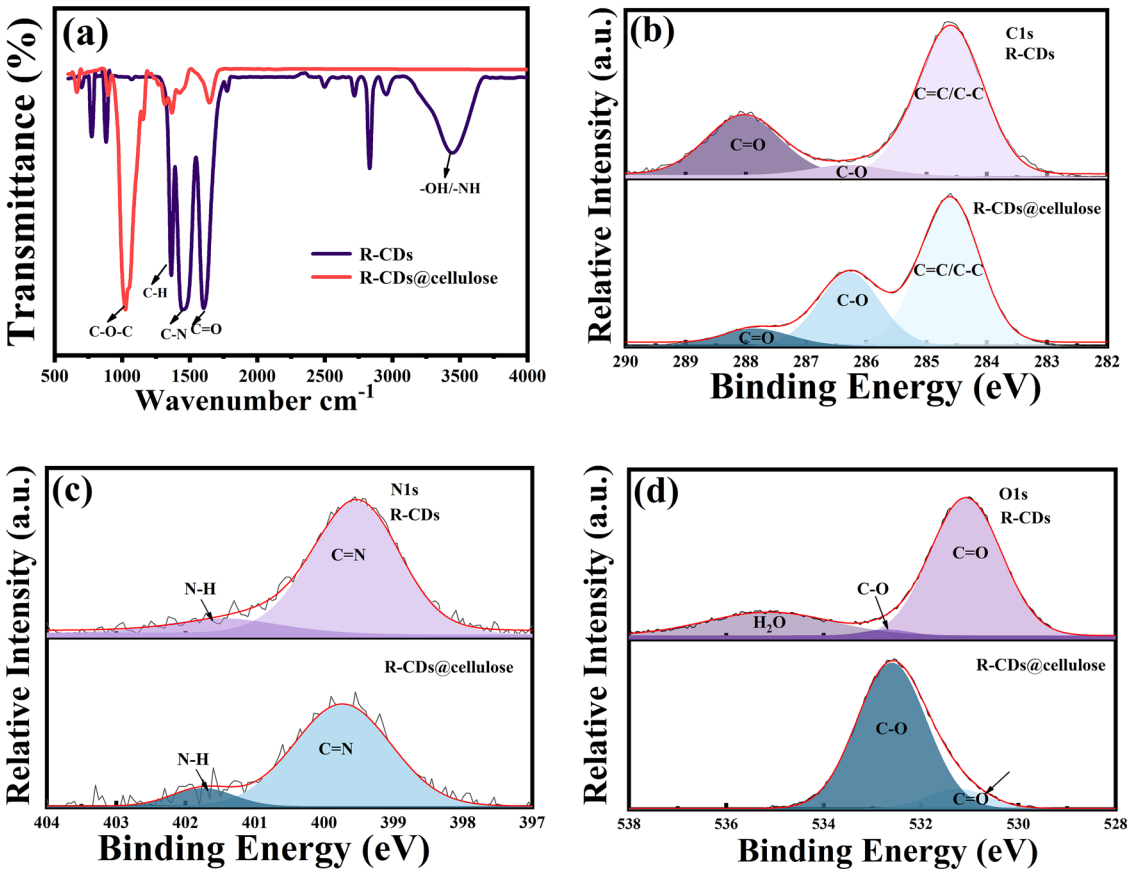


**Figure 2.** (a) FT-IR spectrum and high-resolution XPS spectrum of (b) C 1s, (c) N 1s, and (d) O 1s in R-CDs and R-CDs@cellulose films.

length and width measuring 100 and 50 mm, respectively. The transparent films were treated with boiling water for 20 min and preserved in cool water for further use. R-CDs (0.04 g) were dispersed in 1000 mL of DI water to obtain an R-CD solution, and the regenerated cellulose acetate films were soaked in the solution under vigorous stirring for 3 days until the R-CDs adhered to the films. The obtained transparent reddish films were washed with DI water several times and dried, denoted R-CDs@cellulose.

**2.4. Instruments.** The transmission electron microscopy (TEM) micrograph of carbon dots was obtained using an FEI Tecnai G2 S-Twin transmission electron microscope with a field emission gun operating at 200 kV. The particle-size distribution of R-CDs was measured with a particle size analyzer (Zetasizer Nano ZS, Malvern Instruments Ltd., England). Atomic force microscopy (AFM) images of R-CDs@cellulose were recorded on a Bruker atomic force microscope (Multimode 8) using silicon nitride probes (SNL-10, BRUKER) with a tip radius of 2 nm, spring constant of 0.35 $N{\cdot}m^{-1}$, and resonance frequency of 60 kHz. The UV−vis absorption spectrum of samples was measured with a U-3310 spectrophotometer (Hitachi), and the UV−vis diffuse reflectance spectra (UV−vis DRS) were collected on a UV-3600 plus UV−vis−NIR spectrophotometer with $BaSO_4$ as a reference. The photoluminescence (PL) measurements were conducted utilizing the Hitachi F-7000 spectrophotometer equipped with a 150 W xenon lamp as the excitation source. The persistent decay curves were measured with an FLS980 fluorescence spectrophotometer with a 450 nm pulsed laser as a light source. The X-ray photoelectron spectra (XPS) were collected on a VG ESCALAB MKII electron spectrometer using Mg K$\alpha$ (1200 eV) as the excitation source, while the Fourier transform infrared spectroscopy (FT-IR) results were determined with a Vertex PerkinElmer 580BIR spectrophotometer (Bruker) using the KBr pellet technique.

## 3. RESULTS AND DISCUSSION

**3.1. Structural Characterization of R-CDs and R-CDs@Cellulose Films.** The structural characterizations have been carried out to confirm the morphology and chemical compositions of R-CDs and the R-CDs@cellulose composite. The TEM (Figure 1a) image showed well-dispersed carbon dots of about 6 nm, which corresponded with the size distribution results of 6.15 nm on average, as shown in the inset of Figure 1a. The well-crystallized lattice fringes of 0.21 nm corresponded to the (100) plane of the graphitic intralayer, indicating the successful synthesis of well-crystallized R-CDs. Similar results of R-CD particle heights were revealed by atomic force microscopy (AFM) ranging from 5 to 8 nm, as shown in Figure 1c.

The combination of R-CDs and cellulose films was confirmed by the AFM image. The height image and DMT modulus maps of R-CDs@cellulose films are displayed in Figure 1d,e. The R-CDs decorated unevenly on the surface of the cellulose film was revealed in the AFM height image, while some particles of several nanometers above the films were clearly observed. The size ranging from 4 to 8 nm was in good accordance with that of carbon dots. Also, the DMT modulus maps show large differences between the R-CDs and the cellulose film, and the modulus value of the cellulose film of ∼2 GPa increased sharply to ∼30 GPa when combined with R-


https://doi.org/10.1021/acsomega.1c06426
ACS Omega 2022, 7, 6834−6842

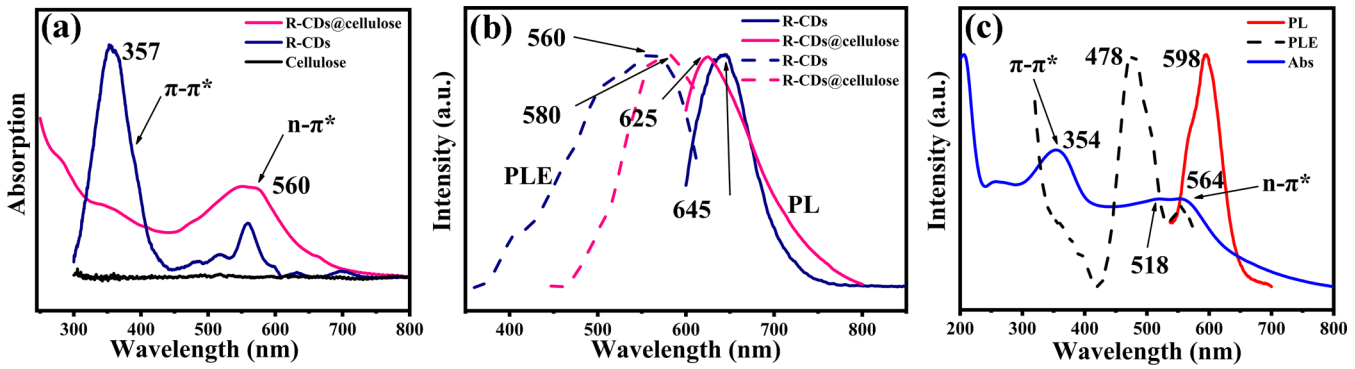


**Figure 3.** (a) Absorption spectra and (b) PL excitation and emission spectra of R-CDs and R-CDs@cellulose films, and (c) absorption, PL excitation, and emission spectra of R-CD powder.

CDs. The difference could be observed in the merged image in Figure 1f.

The combination of R-CDs and cellulose films was further characterized with Fourier transform infrared (FT-IR) spectrum, as shown in Figure 2a. In the purple line of R-CDs, a broad absorption band located at 3100−3500 $cm^{-1}$ was assigned to $\nu$(O−H) and $\nu$(N−H), which afford the hydrophilicity and stability of the R-CDs in an aqueous system.[27] The peak of the $\nu$(C−H) at 2835 $cm^{-1}$ probably resulted from the nongraphitizing carbon chains adhered to the surface of R-CDs.[28] The peaks at 1550−1700 $cm^{-1}$ were attributed to the $\nu$(C═O), and the peaks at 1330−1480 $cm^{-1}$ were assigned to $\delta$(C−H)/$\nu$(C−N).[29] The bands at 752 and 613 $cm^{-1}$ are the characteristic peaks of the C−H out-of-plane bending vibration of aromatic benzene with the phenazine skeleton.[28] When the R-CDs were incorporated into cellulose films, as shown in the red line, two typical bands at 1020 $cm^{-1}$ ascribed to the epoxy group stretching vibration band of C−O−C belonged to the cellulose acetate film substrate.[30]

It can be inferred that after a long reaction in solution, the acetoxy group falls off and is separated in the hydrolysis process of acetic anhydride, and the surface groups of cellulose molecules react with the carboxyl groups in the carbon dots to form chemical bonds. On the other hand, due to the limited number of R-CDs in comparison to films, the hydroxyl and amino groups of R-CDs were scarcely shown. Therefore, the hydroxyl peaks disappeared in the R-CDs@cellulose composite. The C−N and C═O bonding were still detectable in the R-CDs@cellulose film, which was attributed to the presence of carbon dots and the formation of a chemical bond between R-CDs and cellulose films.

The full survey XPS spectrum (Figure S1) of the R-CDs and R-CDs@cellulose films displayed three peaks at 285, 400, and 532 eV, which were assigned to C, N, and O, respectively. The high-resolution XPS spectra of C 1s, N 1s, and O 1s are shown in Figure 2b−d. There were three peaks located at 284.61, 286.31, and 288.01 eV in the C 1s spectrum of the R-CDs, which can be assigned to C−C/C═C, C−O, and C═O, respectively.[7] However, in the R-CDs@cellulose thin film, the binding energy remained almost unchanged (284.6, 286.27, and 287.96 eV). The main peak of C−C/C═C was attributed to the skeleton of cellulose acetate and the carbon core of CDs, while the relative change in the C−O content and C═O content was due to the large addition of cellulose acetate, which showed an overall increase in the C−O content and a decrease in the C═O content, which was in good accordance with the above FT-IR results. In the N 1s spectra of R-CDs and R-CDs@cellulose films, the peaks located at 399.5 and 401.5 eV were attributed to C═N and N−H, respectively. In the N 1s spectra of R-CDs and R-CDs@cellulose films, no obvious relative content change and binding energy shift of the graphitic N and amino N were observed, indicating that the carbon core structure was maintained during the combination. Three peaks located at 531.07, 532.70, and 535.4 eV assigned to C═O, C−O, and adsorbed water, respectively, were observed in the R-CDs.[29] The binding energies of C═O and C−O peaks were identical in the R-CDs@cellulose films, and the content variation of each part was basically consistent with the content of the C 1s spectrum, indicating a successful combination of R-CDs and cellulose films.

**3.2. Optical Properties of R-CDs and R-CD@Cellulose Films.** Furthermore, the optical properties of R-CDs and R-CDs@cellulose films were explored by UV−vis and photoluminescence spectrophotometry. As shown in Figure 3a, two series of absorption bands could be found at 357 and 560 nm in R-CDs, which originated from core absorption and surface absorption, respectively. The core absorption referred to the highest energy level that related to the transition of $sp^2$ carbon domains,[31] while the surface absorption was attributed to the functional groups, especially carbonyl groups here, adhered to the surface of carbon dots. The black baseline showed that the bare cellulose film has no absorption in the 250−800 nm range. The core-state absorption at ∼357 nm and surface-state absorption at ∼560 nm of R-CDs were maintained in the R-CDs@cellulose composite, indicating that the physicochemical properties of R-CDs were unchanged after combining. In addition, various amounts of R-CDs were applied in the combination process, resulting in the same absorption peaks except for the varying intensities, suggesting that the R-CDs were incorporated into the cellulose films in the same way. When the concentration of the R-CD solution reached 0.08 mg/mL, the incorporation into cellulose would be saturated, depending on the limited bonding sites on cellulose films, as shown in Figure S2. As a result, the photoluminescence properties of R-CDs were almost maintained in R-CDs@cellulose films. It can be verified in Figure 3b that R-CDs exhibited a red emission at 645 nm under 560 nm excitation. However, the emission peak of R-CDs@cellulose films blue-shifted a little to 625 nm under 580 nm excitation, which should be attributed to the film environment.[14,32] It is believed that the low saturation of carbon dots loaded on the film reduced the excessive resonance energy transfer from each other, which is considered as the reason for the extra blue shift of the emission.[33] In the R-CDs powder, the peaks located at


https://doi.org/10.1021/acsomega.1c06426
ACS Omega 2022, 7, 6834−6842

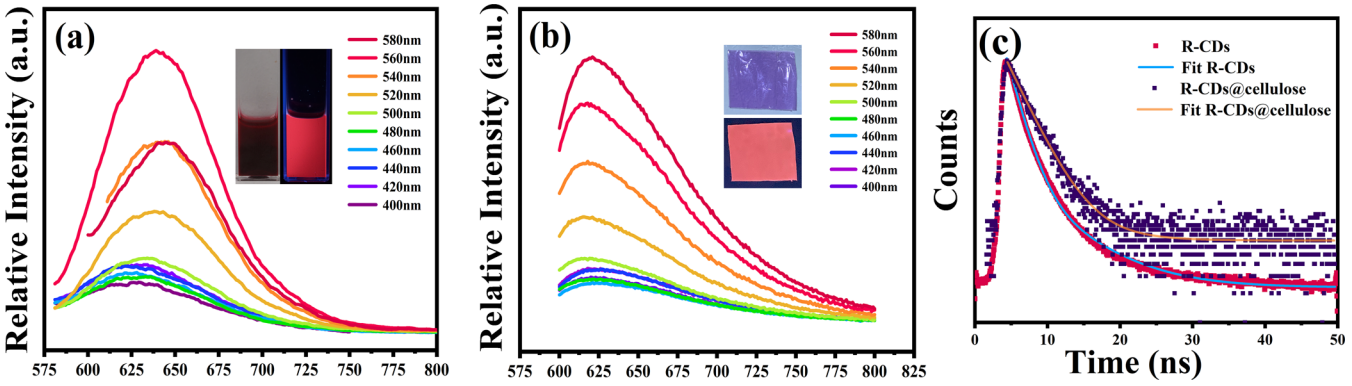


**Figure 4.** (a) Emission spectra of R-CDs and (b) R-CDs@cellulose films with dependent excitation; insets show the photographs of R-CD aqueous solution and R-CDs@cellulose films in daylight and under 365 nm UV excitation. (c) Fluorescence decay curves of R-CDs and R-CDs@cellulose films measured at 450 nm excitation and collected at 620 nm.

354, 518, and 564 nm were attributed to the core state, edge state, and surface state, respectively, which was reported in our previous research,[34] as shown in Figure 3c. However, the signal of the surface state in R-CD powder was greatly weakened due to the aggregation. In addition, the red shift of each peak compared with the dispersed phase was ascribed to the generation of a narrower energy gap caused by the aggregation.[35]

To better understand the optical properties of R-CDs and R-CDs@cellulose films, the excitation-dependent PL spectrum was obtained, as shown in Figure 4. The R-CD solution exhibits a bright red light under UV light irradiation (inset in Figure 4a). With the excitation changing from 400 to 580 nm, the emission intensity of R-CDs increased gradually until the wavelength reached 560 nm and then decreased, while the emission wavelength slightly shifted from 625 to 640 nm and consequently to 645 nm under 580 nm excitation, as shown in Figure 4a. The optimal excitation wavelength corresponds to the surface absorption band in the UV−vis spectrum, indicating that the red fluorescence is attributed to the oxygen-related surface state, namely, the n−$\pi^*$ transitions of C═O bonds from the surface of the R-CDs.[36]

It could be seen that the R-CDs@cellulose films demonstrated an excitation-independent red emission, and 580 nm was the optimized excitation wavelength for R-CDs@cellulose films, as shown in Figure 4b. The excitation-independent phenomenon was due to the small overlap between the excitonic absorption and emission spectrum, which is favorable for efficient fluorescence emission.[37] Considering the carbonyl and amino groups on the surface of R-CDs, the emission of R-CDs should be assigned to a single type of chromophoric structure originating from the surface molecular groups.[37] According to the FT-IR and XPS results above, the formation of chemical bonds between R-CDs and cellulose films essentially changed the surface groups of R-CDs, thus altering the emissive carbonyl-related surface state of R-CDs. On the other hand, the passivation by the cellulose also decreased the surface defect on R-CDs, generating a more effective way for the radiative transition from the surface state. Noteworthily, the emission is quite brighter than that of R-CDs in solution (inset, Figure 4b), and the emission centers were fixed at ∼620 nm due to the combination with cellulose. According to the absolute quantum yield test, the PLQY of R-CDs was 1.23%, which was increased to 5.16% after the combination with cellulose films.

To further investigate the optical properties of R-CDs and R-CDs@cellulose films, the fluorescence lifetimes were measured under an excitation of a 450 nm pulsed laser source, and the emission was monitored at 620 nm. The photoluminescence decays were fitted by a double exponential function; the longer lifetime corresponding to R-CDs@cellulose films was 2.73 ns, and the shorter lifetime corresponding to R-CDs was 1.54 ns, as shown in Figure 4c. Table 1 presents the double exponential fitting parameters of

**Table 1. Amplitudes and Time Constants for Two-Component Exponential Fits for R-CDs and R-CDs@Cellulose Films**

| sample | $\tau_1$ (ns) | $\tau_2$ (ns) | $A_1$ (%) | $A_2$ (%) | $\tau_{avg}$ (ns) |
|---|---|---|---|---|---|
| R-CDs | 1.36 | 4.49 | 84 | 16 | 1.54 |
| RC-CDs | 1.80 | 3.18 | 46 | 54 | 2.73 |

decay curves of R-CDs and R-CDs@cellulose films, where $A_1$ and $A_2$ stand for pre-exponential factors and $\tau_1$ and $\tau_2$ refer to the decay times of each component. A previous study reported that the decreased lifetime should be ascribed to the formation of other nonrecombination channels.[38] Therefore, the $A_1$ fast component constitutes 84% of R-CDs, indicating that the electrons in excited states return to ground states mostly by fast nonradiative-transition processes, resulting in the fast decay lifetime. However, in R-CDs@cellulose films, forming a chemical bond also decreased the surface defect on R-CDs, generating a more effective way for the radiative transition; therefore, the lifetime is longer than that in solution.

Hence, the photoluminescence enhancement and the possible formation process of R-CDs@cellulose films through chemical bonding are demonstrated in Scheme 1. It is well accepted that the interaction among the surface states of the carbon dots is a key factor for the intensity of red emission.[39,40] Hereby, the carboxyl groups were responsible for the red emission of pristine R-CDs according to the UV−vis and PL spectrum. In previous research, carboxyl groups have been confirmed to be present at the surface of carbon dots. And the long-wavelength emissions of carbon dots have been referred to as the carboxyl-related surface states.[41,42] Indeed, the oxygen-containing groups are generally known as the luminescent quenching centers due to a competing transition probability between the activator and the surface recombination centers such as hydroxyl groups,[43,44] which provided nonradiative pathways that caused fluorescence quenching.[45]



https://doi.org/10.1021/acsomega.1c06426
ACS Omega 2022, 7, 6834−6842

**Scheme 1. Schematic Diagram of Possible Chemical Bonding and Fluorescence Mechanism between R-CDs and Cellulose Films**

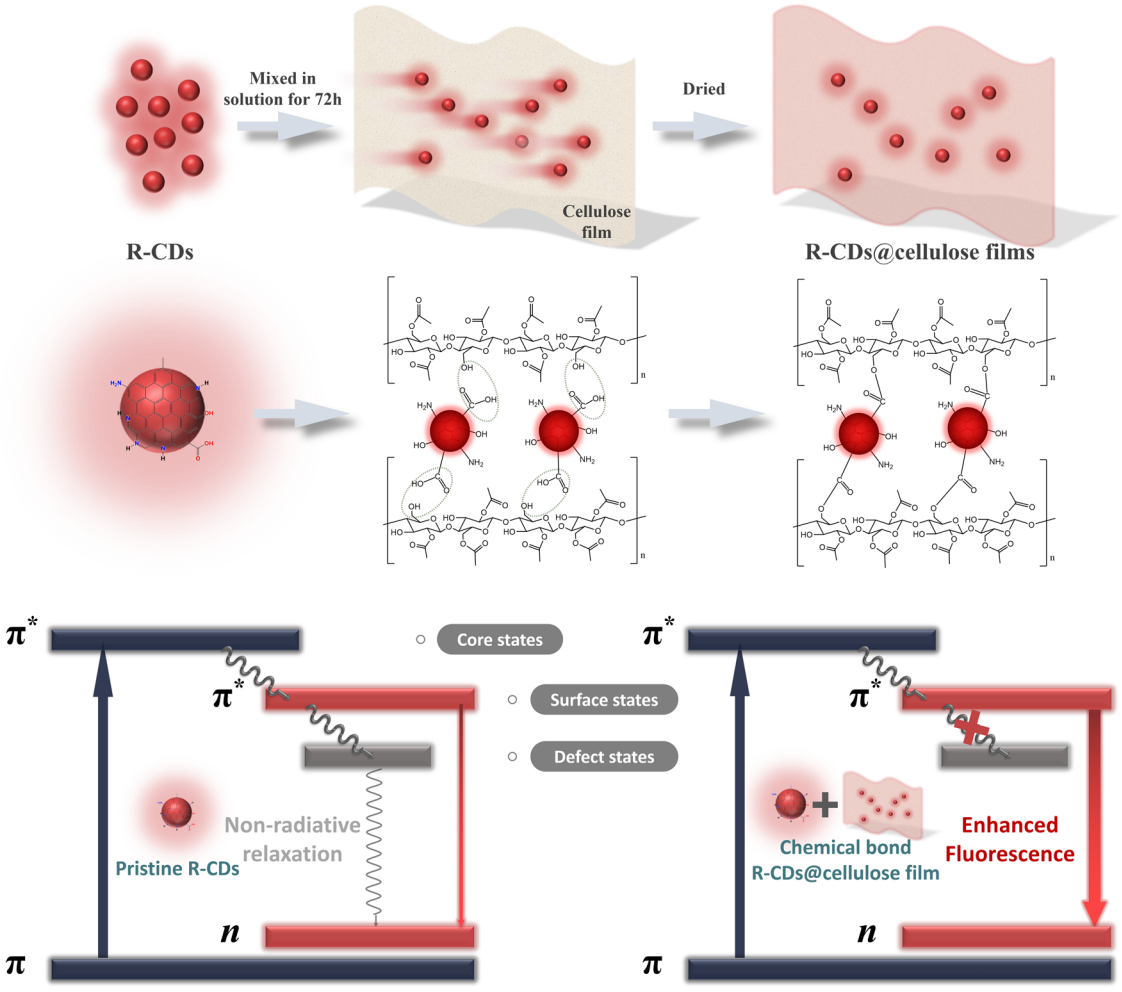


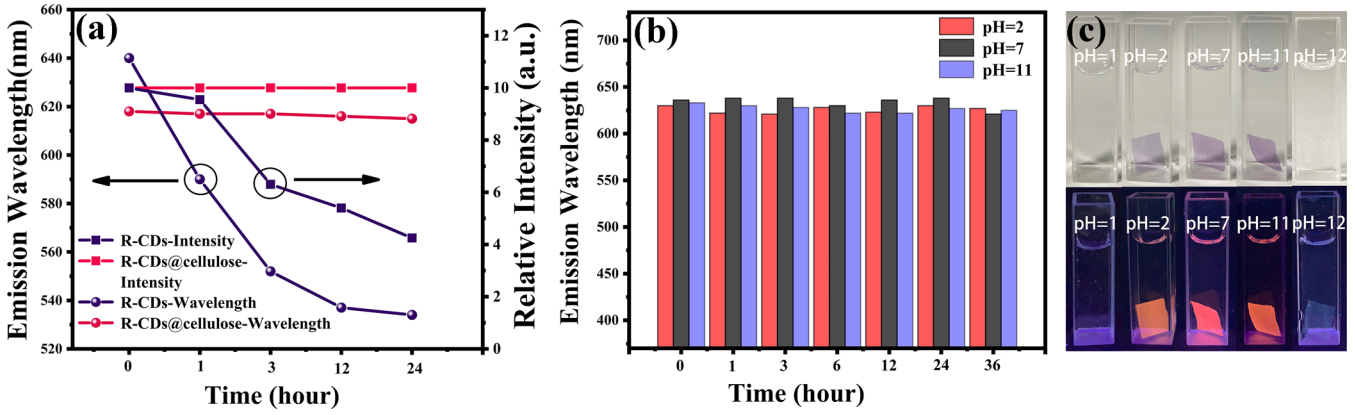


**Figure 5.** (a) Fluorescence intensities and emission wavelengths of R-CDs and R-CDs@cellulose films with various sonication times. (b) Time-dependent emission wavelength change in R-CDs@cellulose films when immersed in different solutions with pH = 2, 7, and 11. (c) Photographs of R-CDs@cellulose films immersed in different solutions with pH = 1, 2, 7, 11, and 12 in daylight and under 365 nm UV excitation.

Therefore, the oxidation of surface groups created in the open air led to the generation of nonradiative defect states, where the surface-state emission was suppressed. According to the above results, the R-CDs suffered from severe energy consumption in defect states through nonradiative relaxation caused by oxygen-related groups, resulting in the low fluorescence efficiency in solution. In contrast, the incorporation of R-CDs into cellulose films established a stable chemical bond utilizing the oxygen-related groups, not only eliminating nonradiative recombination of localized electron−hole pairs but also sealing the efficient radiative process through surface states and thus enhancing the red emission.[46]

**3.3. Stability Testing of R-CDs and R-CDs@Cellulose Films.** Stability is an essential concern during applications.



https://doi.org/10.1021/acsomega.1c06426
ACS Omega 2022, 7, 6834−6842

Therefore, additional time-dependent experiments were performed to evaluate the stability of R-CDs and R-CDs@cellulose films. It is worth noting that the PL intensity of the R-CD solution decreased rapidly when exposed to air, which is probably due to the oxidation of unstable surface functional groups that introduced a large number of defects. In contrast, the fluorescence properties of R-CDs@cellulose films remained unchanged throughout the experiment. It should be noted that both the emission wavelength and intensity remained unchanged even when the R-CDs@cellulose film was exposed to air for 12 months, as shown in Figure S3. It can be concluded that the incorporation of R-CDs into cellulose films replaced the bonding sites for oxygen-related groups that caused nonradiative recombination of localized electron−hole pairs. While the formation of chemical bonds also provided an efficient radiative process and thus enhanced the red emission.[46]

The control time-dependent experimental results are shown in Figure 5a. The R-CD solution was unstable when exposed to open air (purple lines). The emission wavelength blue-shifted from 640 nm to 534 nm, and the PL intensity decreased by 60% during 24 h, as demonstrated in Figure 5a. On the contrary, the R-CDs@cellulose films exhibited ultrastable fluorescence properties. The PL intensity remained stable when exposed to air for 24 h, and the wavelength was scarcely shifted, which can be attributed to the strength of the chemical bond between R-CDs and R-CDs@cellulose films. Since the chemical bond has been confirmed during the combination, the stability of R-CDs@cellulose films in pure water, acidic, and alkaline environments was investigated. A robust test was carried out to immerse R-CDs@cellulose films into pure water, with continuous sonication; even upon rubbing and stretching, the composite expressed a steady characteristic, and the PL properties barely changed after 24 h of treatment, indicating that a chemical bond was formed instead of physical adsorption. Analogously, after 24 h of immersion in pH of 2, 7, and 11, the R-CDs@cellulose films showed a steady emission of about 618 nm, and the intensity scarcely changed, as shown in Figure 5b. This excellent property comes from the nature of cellulose films due to the nanofibrous structure that offered rigidity and dense bonding site for the combination of R-CDs. However, when the pH was adjusted to 1, the cellulose was dissolved, resulting in the deformation of the film, thus quenching the R-CDs@cellulose composite. In contrast, when the pH was adjusted to 12, the chemical bond between R-CDs and cellulose films was destroyed and the fluorescence of R-CDs was quenched immediately, while the structure of cellulose was maintained. Thus, the cellulose films as a supporter could provide protection for R-CDs from quenching in weak acid−base environments by means of chemical bonding.

## 4. CONCLUSIONS

In this work, a red-emissive carbon dot-based nanocomposite was synthesized through chemical bonding with cellulose films. Structural characterization confirmed that the acetoxy group falls off and is separated in the hydrolysis process, and the surface groups of cellulose molecules react with the carboxyl groups in the carbon dots to form chemical bonds. The 640 nm red emission originating from the surface states of R-CDs was maintained in R-CDs@cellulose films with a slight blue shift to 618 nm due to the film environment. The formation of chemical bonding between R-CDs and cellulose films is the key point of PL enhancement and stability improvement. This strategy not only eliminated the nonradiative recombination of localized electron−hole pairs in defect states originating from the oxygen-related groups but also preserved the efficient radiative process through surface states and thus enhanced the PLQY over 4 times. Due to the stable chemical bonding, the R-CDs@cellulose composite exhibited invariable PL intensity and wavelength for 12 months. And the R-CDs@cellulose films showed outstanding stability either in water with mechanical interference or weak acid−base environments under pHs ranging from 2 to 11, which provided the R-CD composite a wide spectrum of optical applications of carbon dots and a promising future in solid-state lighting.

## ■ ASSOCIATED CONTENT

### Supporting Information

The Supporting Information is available free of charge at https://pubs.acs.org/doi/10.1021/acsomega.1c06426.

Full survey XPS spectrum of R-CDs and R-CDs@cellulose films; absorption spectrum of R-CDs@cellulose films with different concentrations of carbon dots; and the photoluminescence intensity of R-CDs@cellulose films tested after synthesis for 1−12 months when exposed in the open air (Figures S1−S3) (PDF)

## ■ AUTHOR INFORMATION


### Corresponding Authors

**Yeqing Chen** − *School of Applied Physics and Materials, Wuyi University, Jiangmen 529020 Guangdong, P. R. China;* orcid.org/0000-0001-6090-1669; Email: yqchenwyu@126.com

**Mingxuan Cao** − *Faculty of Intelligent Manufacturing, Wuyi University, Jiangmen 529020 Guangdong, P. R. China;* orcid.org/0000-0002-9800-1460; Email: mingxuancao@tju.edu.cn

### Authors

**Gaoyang Xiong** − *School of Applied Physics and Materials, Wuyi University, Jiangmen 529020 Guangdong, P. R. China*

**Lina Zhu** − *School of Applied Physics and Materials, Wuyi University, Jiangmen 529020 Guangdong, P. R. China*

**Jie Huang** − *School of Applied Physics and Materials, Wuyi University, Jiangmen 529020 Guangdong, P. R. China*

**Xueying Chen** − *School of Applied Physics and Materials, Wuyi University, Jiangmen 529020 Guangdong, P. R. China*

**Yan Chen** − *School of Applied Physics and Materials, Wuyi University, Jiangmen 529020 Guangdong, P. R. China*

Complete contact information is available at: https://pubs.acs.org/10.1021/acsomega.1c06426


### Notes

The authors declare no competing financial interest.

## ■ ACKNOWLEDGMENTS

This work was supported by the Guangdong Province Key Field R&D Program Project (2020B090922004), National Natural Science Foundation of China (Grant No. 51802228), Science Foundation for Young Teachers of Wuyi University (No. 2019td03), Jiangmen City Fundamental and Applied Fundamental Research Fund (2020030102130005402), Special Projects in Key Fields of Guangdong Universities

(2021ZDZX1022), and Guangdong Provincial College Innovation Team Project (2021KCXTD042).

## REFERENCES

(1) Chen, B. B.; Liu, M. L.; Zhan, L.; Li, C. M.; Huang, C. Z. Terbium(III) Modified Fluorescent Carbon Dots for Highly Selective and Sensitive Ratiometry of Stringent. *Anal. Chem.* **2018**, *90*, 4003−4009.
(2) Zhang, Y.; Nie, Y.; Zhu, R.; Han, D.; Zhao, H.; Li, Z. Nitrogen doped carbon dots for turn-off fluorescent detection of alkaline phosphatase activity based on inner filter effect. *Talanta* **2019**, *204*, 74−81.
(3) Gao, G.; Jiang, Y.-W.; Jia, H.-R.; Yang, J.; Wu, F.-G. On-off-on fluorescent nanosensor for $Fe^{3+}$ detection and cancer/normal cell differentiation via silicon-doped carbon quantum dots. *Carbon* **2018**, *134*, 232−243.
(4) Jiang, K.; Sun, S.; Zhang, L.; Lu, Y.; Wu, A.; Cai, C.; Lin, H. Red, green, and blue luminescence by carbon dots: full-color emission tuning and multicolor cellular imaging. *Angew. Chem., Int. Ed.* **2015**, *54*, 5360−5363.
(5) Zhou, N.; Hao, Z.; Zhao, X.; Maharjan, S.; Zhu, S.; Song, Y.; Yang, B.; Lu, L. A novel fluorescent retrograde neural tracer: cholera toxin B conjugated carbon dots. *Nanoscale* **2015**, *7*, 15635−15642.
(6) Yuan, F.; Yuan, T.; Sui, L.; Wang, Z.; Xi, Z.; Li, Y.; Li, X.; Fan, L.; Tan, Z.; Chen, A.; Jin, M.; Yang, S. Engineering triangular carbon quantum dots with unprecedented narrow bandwidth emission for multicolored LEDs. *Nat. Commun.* **2018**, *9*, No. 2249.
(7) Feng, T.; Zeng, Q.; Lu, S.; Yan, X.; Liu, J.; Tao, S.; Yang, M.; Yang, B. Color-Tunable Carbon Dots Possessing Solid-State Emission for Full-Color Light-Emitting Diodes Applications. *ACS Photonics* **2018**, *5*, 502−510.
(8) Ye, X.; Xiang, Y.; Wang, Q.; Li, Z.; Liu, Z. A Red Emissive Two-Photon Fluorescence Probe Based on Carbon Dots for Intracellular pH Detection. *Small* **2019**, *15*, No. 1901673.
(9) Malina, T.; Poláková, K.; Skopalík, J.; Milotová, V.; Holá, K.; Havrdová, M.; Tománková, K. B.; Čmiel, V.; Šefc, L.; Zbořil, R. Carbon dots for in vivo fluorescence imaging of adipose tissue-derived mesenchymal stromal cells. *Carbon* **2019**, *152*, 434−443.
(10) Geng, X.; Sun, Y.; Li, Z.; Yang, R.; Zhao, Y.; Guo, Y.; Xu, J.; Li, F.; Wang, Y.; Lu, S.; Qu, L. Retrosynthesis of Tunable Fluorescent Carbon Dots for Precise Long-Term Mitochondrial Tracking. *Small* **2019**, *15*, No. 1901517.
(11) Fang, X.; Ding, J.; Yuan, N.; Sun, P.; Lv, M.; Ding, G.; Zhu, C. Graphene quantum dot incorporated perovskite films: passivating grain boundaries and facilitating electron extraction. *Phys. Chem. Chem. Phys.* **2017**, *19*, 6057−6063.
(12) Han, Z.; Wang, K.; Du, F.; Yin, Z.; Xie, Z.; Zhou, S. High efficiency red emission carbon dots based on phenylene diisocyanate for trichromatic white and red LEDs. *J. Mater. Chem. C* **2018**, *6*, 9631−9635.
(13) Liu, Y.; Duan, W.; Song, W.; Liu, J.; Ren, C.; Wu, J.; Liu, D.; Chen, H. Red Emission B, N, S-co-Doped Carbon Dots for Colorimetric and Fluorescent Dual Mode Detection of Fe(3+) Ions in Complex Biological Fluids and Living Cells. *ACS Appl. Mater. Interfaces* **2017**, *9*, 12663−12672.
(14) Dong, X. Y.; Niu, X. Q.; Zhang, Z. Y.; Wei, J. S.; Xiong, H. M. Red Fluorescent Carbon Dot Powder for Accurate Latent Fingerprint Identification using an Artificial Intelligence Program. *ACS Appl. Mater. Interfaces* **2020**, *12*, 29549−29555.
(15) He, Y.; He, J.; Wang, L.; Yu, Z.; Zhang, H.; Liu, Y.; Lei, B. Synthesis of double carbon dots co-doped mesoporous Al2O3 for ratiometric fluorescent determination of oxygen. *Sens. Actuators, B* **2017**, *251*, 918−926.
(16) Zhu, S.; Wang, L.; Zhou, N.; Zhao, X.; Song, Y.; Maharjan, S.; Zhang, J.; Lu, L.; Wang, H.; Yang, B. The crosslink enhanced emission (CEE) in non-conjugated polymer dots: from the photoluminescence mechanism to the cellular uptake mechanism and internalization. *Chem. Commun.* **2014**, *50*, 13845−13848.
(17) Zhai, Y.; Wang, Y.; Li, D.; Zhou, D.; Jing, P.; Shen, D.; Qu, S. Red carbon dots-based phosphors for white light-emitting diodes with color rendering index of 92. *J. Colloid Interface Sci.* **2018**, *528*, 281−288.
(18) Wang, C.; Hu, T.; Chen, Y.; Xu, Y.; Song, Q. Polymer-Assisted Self-Assembly of Multicolor Carbon Dots as Solid-State Phosphors for Fabrication of Warm, High-Quality, and Temperature-Responsive White-Light-Emitting Devices. *ACS Appl. Mater. Interfaces* **2019**, *11*, 22332−22338.
(19) Sun, C.; Zhang, Y.; Sun, K.; Reckmeier, C.; Zhang, T.; Zhang, X.; Zhao, J.; Wu, C.; Yu, W. W.; Rogach, A. L. Combination of carbon dot and polymer dot phosphors for white light-emitting diodes. *Nanoscale* **2015**, *7*, 12045−12050.
(20) Li, Y.; Miao, P.; Zhou, W.; Gong, X.; Zhao, X. N-doped carbon-dots for luminescent solar concentrators. *J. Mater. Chem. A* **2017**, *5*, 21452−21459.
(21) Wang, Y.; Kalytchuk, S.; Wang, L.; Zhovtiuk, O.; Cepe, K.; Zboril, R.; Rogach, A. L. Carbon dot hybrids with oligomeric silsesquioxane: solid-state luminophores with high photoluminescence quantum yield and applicability in white light emitting devices. *Chem. Commun.* **2015**, *51*, 2950.
(22) Kim, T. H.; Wang, F.; Mccormick, P.; Wang, L.; Brown, C.; Li, Q. Salt-embedded carbon nanodots as a UV and thermal stable fluorophore for light-emitting diodes. *J. Lumin.* **2014**, *154*, 1−7.
(23) Zhou, D.; Li, D.; Jing, P.; Zhai, Y.; Shen, D.; Qu, S.; Rogach, A. L. Conquering Aggregation-Induced Solid-State Luminescence Quenching of Carbon Dots through a Carbon Dots-Triggered Silica Gelation Process. *Chem. Mater.* **2017**, *29*, 1779−1787.
(24) Zhou, D.; Zhai, Y.; Qu, S.; Li, D.; Jing, P.; Ji, W.; Shen, D.; Rogach, A. L. Electrostatic Assembly Guided Synthesis of Highly Luminescent Carbon-Nanodots@$BaSO_4$ Hybrid Phosphors with Improved Stability. *Small* **2017**, No. 1602055.
(25) Sun, Y.; Liu, J.; Pang, X.; Zhang, X.; Zhuang, J.; Zhang, H.; Hu, C.; Zheng, M.; Lei, B.; Liu, Y. Temperature-responsive conversion of thermally activated delayed fluorescence and room-temperature phosphorescence of carbon dots in silica. *J. Mater. Chem. C* **2020**, *8*, 5744−5751.
(26) Ding, H.; Wei, J. S.; Zhong, N.; Gao, Q. Y.; Xiong, H. M. Highly Efficient Red-Emitting Carbon Dots with Gram-Scale Yield for Bioimaging. *Langmuir* **2017**, *33*, 12635−12642.
(27) Qu, S.; Wang, X.; Lu, Q.; Liu, X.; Wang, L. A biocompatible fluorescent ink based on water-soluble luminescent carbon nanodots. *Angew. Chem., Int. Ed.* **2012**, *51*, 12215−12218.
(28) Liu, J.; Li, D.; Zhang, K.; Yang, M.; Sun, H.; Yang, B. One-Step Hydrothermal Synthesis of Nitrogen-Doped Conjugated Carbonized Polymer Dots with 31% Efficient Red Emission for In Vivo Imaging. *Small* **2018**, *14*, No. 1703919.
(29) Li, D.; Han, D.; Qu, S. N.; Liu, L.; Jing, P. T.; Zhou, D.; Ji, W. Y.; Wang, X. Y.; Zhang, T. F.; Shen, D. Z. Supra-(carbon nanodots) with a strong visible to near-infrared absorption band and efficient photothermal conversion. *Light: Sci. Appl.* **2016**, *5*, No. e16120.
(30) Yuan, F.; Ding, L.; Li, Y.; Li, X.; Fan, L.; Zhou, S.; Fang, D.; Yang, S. Multicolor fluorescent graphene quantum dots colorimetrically responsive to all-pH and a wide temperature range. *Nanoscale* **2015**, *7*, 11727−11733.
(31) Miao, X.; Yan, X.; Qu, D.; Dabing, L.; Ta, F. F.; Su, Z. Red Emissive Sulfur, Nitrogen Codoped Carbon Dots and Their Application in Ion Detection and Theraonostics. *ACS Appl. Mater. Interfaces* **2017**, *9*, 18549−18556.
(32) Liu, Y.; Wang, P.; Fernando, K. A. S.; Lecroy, G. E.; Maimaiti, H.; Harruff-Miller, B.; Lewis, W.; Bunker, C. E.; Hou, Z. L.; Sun, Y. P. Enhanced fluorescence properties of carbon dots in polymer films. *J. Mater. Chem. C* **2016**, *4*, 6967−6974.
(33) Chen, Y.; et al. A Self-Quenching-Resistant Carbon-Dot Powder with Tunable Solid-State Fluorescence and Construction of Dual-Fluorescence Morphologies for White Light-Emission. *Adv. Mater.* **2016**, *28*, 312−318.
(34) Chen, Y.; Lian, H.; Wei, Y.; He, X.; Chen, Y.; Wang, B.; Zeng, Q.; Lin, J. Concentration-induced multi-colored emissions in carbon


https://doi.org/10.1021/acsomega.1c06426
ACS Omega 2022, 7, 6834−6842

dots: origination from triple fluorescent centers. *Nanoscale* **2018**, *10*, 6734−6743.
(35) He, W.; Weng, W.; Sun, X.; Pan, Y.; Chen, X.; Liu, B.; Shen, J. Multifunctional Carbon Dots with Solid−Liquid State Orange Light Emission for Vitamin B12 Sensing, Cellular Imaging, and Red/White Light-Emitting Diodes. *ACS Appl. Nano Mater.* **2020**, *3*, 7420−7427.
(36) Nguyen, H. A.; Srivastava, I.; Pan, D.; Gruebele, M. Unraveling the Fluorescence Mechanism of Carbon Dots with Sub-Single-Particle Resolution. *ACS Nano* **2020**, *14*, 6127−6137.
(37) Zhang, X.; et al. Self-Quenching-Resistant Red Emissive Carbon Dots with High Stability for Warm White Light-Emitting Diodes with a High Color Rendering Index. *Adv. Opt. Mater.* **2020**, *8*, No. 2000251.
(38) Zhou, Z.; Tian, P.; Liu, X.; Mei, S.; Zhou, D.; Li, D.; Jing, P.; Zhang, W.; Guo, R.; Qu, S.; Rogach, A. L. Hydrogen Peroxide-Treated Carbon Dot Phosphor with a Bathochromic-Shifted, Aggregation-Enhanced Emission for Light-Emitting Devices and Visible Light Communication. *Adv. Sci.* **2018**, *5*, No. 1800369.
(39) Kundelev, E. V.; Tepliakov, N. V.; Leonov, M. Y.; Maslov, V. G.; Rogach, A. L.; et al. Toward Bright Red-Emissive Carbon Dots through Controlling Interaction among Surface Emission Centers. *J. Phys. Chem. Lett.* **2020**, *11*, 8121−8127.
(40) Miao, X.; Qu, D.; Yang, D.; Nie, B.; Zhao, Y.; Fan, H.; Sun, Z. Photoluminescence: Synthesis of Carbon Dots with Multiple Color Emission by Controlled Graphitization and Surface Functionalization. *Adv. Mater.* **2018**, *30*, No. 1870002.
(41) Miao, X.; Qu, D.; Yang, D.; Nie, B.; Zhao, Y.; Fan, H.; Sun, Z. Synthesis of Carbon Dots with Multiple Color Emission by Controlled Graphitization and Surface Functionalization. *Adv. Mater.* **2018**, *30*, No. 1704740.
(42) Zhu, J.; Bai, X.; Chen, X.; Xie, Z.; Zhu, Y.; Pan, G.; Zhai, Y.; Zhang, H.; Dong, B.; Song, H. Carbon dots with efficient solid-state red-light emission through the step-by-step surface modification towards light-emitting diodes. *Dalton Trans.* **2018**, *47*, 3811−3818.
(43) Wu, M.; Park, H.; Lee, E. G.; Lee, S.; Hong, Y. J.; Choi, S. Luminescence Quenching Behavior of Hydrothermally Grown YVO4:Eu3+ Nanophosphor Excited under Low Temperature and Vacuum Ultra Violet Discharge. *Materials* **2020**, *13*, 3270.
(44) Langlet, M.; Coutier, C.; Fick, J.; Audier, M.; Meffre, W.; Jacquier, B.; Rimet, R. Sol−gel thin film deposition and characterization of a new optically active compound: $Er_2Ti_2O_7$. *Opt. Mater.* **2001**, *16*, 463−473.
(45) Sun, C.; Zhang, Y.; Sun, K.; Reckmeier, C.; Zhang, T.; Zhang, X.; Zhao, J.; Wu, C.; Yu, W. W.; Rogach, A. L. Combination of carbon dot and polymer dot phosphors for white light-emitting diodes. *Nanoscale* **2015**, *7*, 12045−12050.
(46) Zhu, J.; Bai, X.; Zhai, Y.; Chen, X.; Zhu, Y.; Pan, G.; Zhang, H.; Dong, B.; Song, H. Carbon dots with efficient solid-state photoluminescence towards white light-emitting diodes. *J. Mater. Chem. C* **2017**, *5*, 11416−11420.


https://doi.org/10.1021/acsomega.1c06426
*ACS Omega* 2022, 7, 6834−6842